

Article

# Thermal Stability and Performance Testing of Oil-based CuO Nanofluids for Solar Thermal Applications

Moucun Yang <sup>1</sup>, Sa Wang <sup>1</sup>, Yuezhao Zhu <sup>1</sup>, Robert A. Taylor <sup>2,\*</sup> , M.A. Moghimi <sup>3</sup>   
and Yinfeng Wang <sup>1</sup>

<sup>1</sup> School of Mechanical and Power Engineering, Nanjing Tech University, Nanjing, China, 30 Puzhu South Rd, Pukou, Nanjing 211816, China; young\_2004@njtech.edu.cn (M.Y.); wangsa940425@163.com (S.W.); zyz@njtech.edu.cn (Y.Z.); wangyf@njtech.edu.cn (Y.W.)

<sup>2</sup> School of Mechanical and Manufacturing Engineering/School of Photovoltaic and Renewable Energy Engineering, University of New South Wales, Gate 14, Barker St., Kensington, Sydney, NSW 2052, Australia

<sup>3</sup> Department of Design and Engineering, Staffordshire University, Stoke-On-Trent ST4 2DE, UK; Mohammad.Moghimi-Ardekani@staffs.ac.uk

\* Correspondence: robert.taylor@unsw.edu.au; Tel.: +61-2-9385-5400

Received: 15 January 2020; Accepted: 12 February 2020; Published: 17 February 2020



**Abstract:** For solar thermal systems, nanofluids have been proposed as working fluids due to their enhanced optical and thermal properties. However, nanoparticles may agglomerate over time, heating and thermal cycles. Even though pristine nanofluids have proven to enhance performance in low-temperature applications, it is still unclear if nanofluids can meet the reliability requirements of solar thermal applications. For this aim, the present study conducted experiments with several formulations of oil-based CuO nanofluids in terms of their maximum operational temperatures and their stabilities upon cyclic heating. In the samples tested, the maximum temperature ranged from 80 to 150 °C, and the number of heating cycles ranged from 5 to 45, with heating times between 5 to 60 min. The results showed that heating temperature, heating cycles, and heating time all exacerbated agglomeration of samples. Following these experiments, orthogonal experiments were designed to improve the preparation process and the resultant thermal-impulse stability. Thermal properties of these samples were characterized, and thermal performance in an “on-sun” linear Fresnel solar collector was measured. All tests revealed that thermal performance of a solar collecting system could be enhanced with nanofluids, but thermal stability still needs to be further improved for industrial applications.

**Keywords:** oil-based CuO nanofluids; two-step preparing method; medium temperature; thermal impulse stability; orthogonal experiment

## 1. Introduction

Solar energy has become a global priority to replace conventional fossil fuels in response to worldwide energy supply and environmental concerns [1–3]. As one slice of the energy “pie”, solar thermal collectors can be implemented to harvest useful heat from sunlight for a range of residential and industrial thermal energy needs. To compete with fossil fuels for these applications, solar thermal collectors must be designed to be reliable, cost-effective and to have good optical and thermal performance [4]. Direct absorption solar collectors, the working fluids of which engineered nanoparticles are suspended in, have been a growing area for research and development, due to the fact that it is possible to enhance optical and thermal properties of a solar thermal collector [5]. Along these lines, several recent research papers have demonstrated that nanofluids were able to

improve the efficiency of solar thermal collectors [6]. For example, the thermal efficiency of a flat-plate solar collector was improved by about 28.3% with 0.2 wt %  $\text{Al}_2\text{O}_3/\text{H}_2\text{O}$  nanofluids [7], and for a PV/T (photovoltaic/thermal) collector with 3.0 wt %  $\text{SiO}_2/\text{H}_2\text{O}$  nanofluids, a 12.8% thermal efficiency enhancement was reported [8]. A 10% improvement was reported for solar tower power collectors with 0.001 wt % graphite nanofluids [9].

However, most of these studies use freshly prepared nanofluids and neglect the fact that nanoparticles may agglomerate over service time, degrading their optical and thermal performance. A great number of studies reported stability of nanofluids for these applications was mainly related to the preparation processes, such as temperature [10], ultrasonication time [11,12], type of dispersant (surfactant) [13,14], particle size [15], nanoparticles' concentrations [16,17], base fluids [18], pH levels [19,20], and protective shells of nanoparticles [21]. Long-term room-temperature stability has been realized for most nanofluids, such as up to eight-month ethanol-based multiwalled carbon nanotube (MWCNT) nanofluids [22]. Overall, the current literatures on stability seem to focus mostly on parameters involved in preparing fluids rather than on real applications' operational conditions, such as working temperature, thermal impulse intensity, and the number of heating cycles.

Thus, studying performance under operational conditions represents a not well-understood, but critical, factor of suspension stability. This is especially true for solar applications, where the working fluids will continually experience medium or high temperatures [23] (e.g., in a linear Fresnel collector [24]). Thus, there is a pressing need to extend stability investigations into medium- or high-temperature ranges. Sani et al. [25] studied particle aggregation over five cycles of heating and cooling for water-based suspensions. For temperatures up to 120 °C, they observed good stability, but at higher temperatures (up to 150 °C), some aggregation was detected. Hordy et al. [22] carried out an experimental study on nanofluids at medium temperatures, and it was demonstrated that water- and glycol-based nanofluids were heated to 85 and 170 °C, respectively, without any observable agglomeration. However, the Therminol<sup>®</sup> VP-1 based MWCNT nanofluids showed significant agglomeration after only five thermal cycles. Mesgari [26] studied the thermal stability of plasma and acid-functionalized MWCNT nanofluids in different alkaline fluids. The results showed that the MWCNT nanofluids remained stable at 150 °C. However, there was no further investigation on long-term stability with heating cycles. Jiang investigated the nanofluids stability at medium temperatures by measuring the effective thermal conductivity over time. The results showed that the thermal conductivity decreased when temperature increased from 30 to 210 °C, which may result from nanoparticle aggregation [27]. In addition, working fluids also suffers from the effects of "heating-cooling-heating" thermal cycles due to the use of a heat exchanger. Taking this factor into account, Otanicar et al. [28] conducted an experiment to test the thermal cycles of  $\text{SiO}_2/\text{Au}$  core-shell nanofluids to determine the degree of particle agglomeration generated by 200 accelerated heating cycles with temperatures ranging from 25 to 80 °C. An amount of soft agglomeration in a range of  $\pm 20\%$  was found, and it was possible to reversibly break up agglomerates with regular sonication. Taylor et al. [21] compared the thermal stability of uncoated and coated Ag nanodisc nanofluids. The results showed that even uncoated Ag could resist initial heating (up to 80 °C) while it rapidly agglomerated after several heating cycles. While useful, this temperature range was limited relative to systems that operated well above 100 °C.

It can be inferred from the above that, while there has been some initial promising work towards achieving stable nanofluids for solar collectors, there is still quite a bit of work to be done to move from laboratory stability testing to commercial product reliability. One of the gaps in knowledge stems from the fact that a great deal of nanofluids research focuses on water-based nanofluids for low-temperature ( $\leq 100$  °C) applications [29–31]. However, since a huge demand exists in the medium-temperature range (requiring temperatures just above 100 °C), it is desirable to develop nanofluids, which can use heat transfer oils as their base fluids [32,33]. For these types of nanofluids, only some preliminary "heating" and "heating-cooling-heating" investigations on thermophysical properties have been

conducted [4,34]. Thus, more extensive thermal stability studies of oil-based nanofluids for solar thermal applications need to be conducted to bridge the research gap.

To address this, the thermal stability of CuO/oil nanofluids (prepared by a “two-step” method) was investigated by exposing them to the actual working conditions of a collector system, including the maximum operation temperature, intense thermal impulses, and numerous thermal cycles. Factors, including dispersant type, concentration, and ultrasonic dispersing time, were investigated, and an orthogonal experiment was designed to optimize the preparation process. In addition, the thermal performance of the final CuO/oil nanofluids was tested “on-sun” in a concentrating (linear Fresnel) solar collector.

Thus, the rest of the paper is organized as follows. Section 1 contains a nanofluids preparation process along with the effects of different process parameters on thermal shock stability. Section 2 describes the process for the optimization of a preparation technique. Section 3 describes the thermal properties testing for CuO/oil nanofluids and the associated results. Section 4 contains conclusions.

## 2. Thermal Impulse Stability

The basic objective of putting nanofluids into a solar collecting system is to improve thermal performance. Due to the heat exchange process between nanofluids (the working fluids of a closed collector loop) and a working fluid for thermal applications, nanofluids will rapidly cycle between high and low temperatures (i.e., thermal impulses), and their thermal stability could deteriorate over time. To investigate this effect, CuO/oil nanofluids were prepared and subjected to thermal impulse tests to evaluate their suspension stability. Orthogonal tests of preparation processes were designed to improve stability. The thermal conductivity and photothermal conversion performance were measured to show changes in their performance and, ultimately, their potential for medium-temperature solar-collecting systems. The research approach is shown in Figure 1.

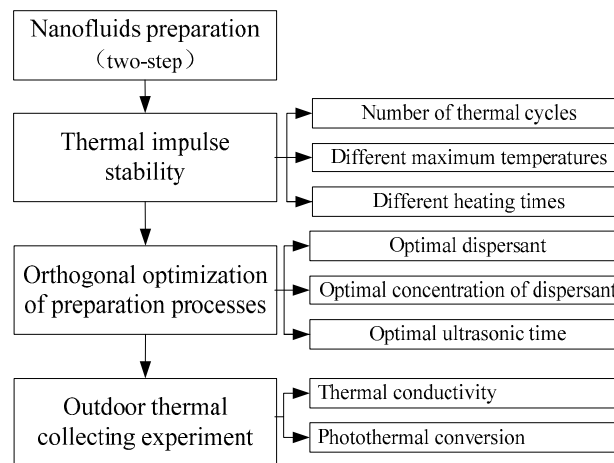


**Figure 1.** Research approach (flowchart).

### 2.1. Nanofluids Preparation

CuO/oil nanofluids were prepared via a “two-step” method (dispersing the CuO powder into a synthetic heat transfer oil, Diphyl DT base fluid from Lanxess Deutschland GmbH, Germany). The spherical CuO nanoparticles were manufactured by Emperor Nanomaterial Co. LTD, China. A TEM image of the dry CuO nanoparticles is shown in Figure 2, displaying particle clustering and (perhaps) particle sintering. The physical properties of CuO and Diphyl DT are shown in Table 1.

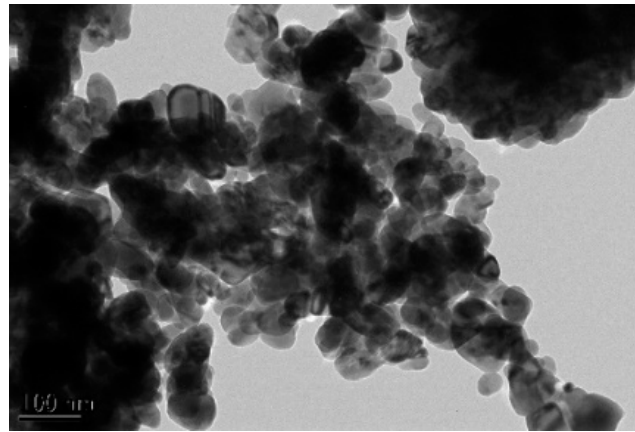


**Figure 2.** TEM image of CuO (mean diameter: 60 nm).

**Table 1.** Physical properties of the base fluid and CuO nanoparticles.

Materials	Mean Diameter, (nm)	Specific Surface, (m <sup>2</sup> /g)	Density, (g/cm <sup>3</sup> )	Thermal Conductivity, (W/(m × K))
Diphyl DT	-	-	1.035	0.1554
CuO	60	60	6.4	76.5

The mass of CuO nanoparticles required to achieve a given percentage of volume concentration in the nanofluids was estimated from Equation (1) [35]:

$$\varphi = \frac{(m/\rho)_{\text{CuO}}}{(m/\rho)_{\text{CuO}} + (m/\rho)_{\text{oil}}}, \quad (1)$$

where  $\varphi$  is the percentage of volume concentration, and  $m$  and  $\rho$  are the mass and density, respectively.

Each nanofluids sample was prepared by adding a measured mass of nanoparticles to a 100 mL volume of the oil base fluid. One milliliter of oleic acid (a dispersant) was added to the mixture inside an ultrasonic bath, which was heated in a stage at 70 and 90 °C for 20 min with periodic stirring. The detailed process is shown in Figure 3a. Note that the process with solid lines is used in almost all reported “two-step” synthesis methods [23] while dashed lines indicate steps taken in this study, which may improve the final stability. A three-day settling test was conducted for a comparison between a “conventional” two-step method and the method with additional steps, with the resultant CuO/oil nanofluids pictured in Figure 3b. It is obvious that, through visual inspection after such a settling test, the stability of CuO/oil nanofluids was improved with additional steps. The additional steps are shown as follows.

1. Soft aggregation of CuO nanoparticles, which occurred during storage/transportation over time at room temperature, can be broken up with about 15 min ultrasonic vibration.
2. Oleic acid (the dispersant) was much less viscous and soluble with the heat transfer oil, when the suspension was heated up to 70 °C. Thus, in this step, the dispersant was added and kept warm for one hour to ensure CuO nanoparticles to fully adsorb oleic acid.
3. The final heating step was also maintained at 90 °C for one hour to ensure the low viscosity of the Diphyl DT during the final stirring/sonication step.

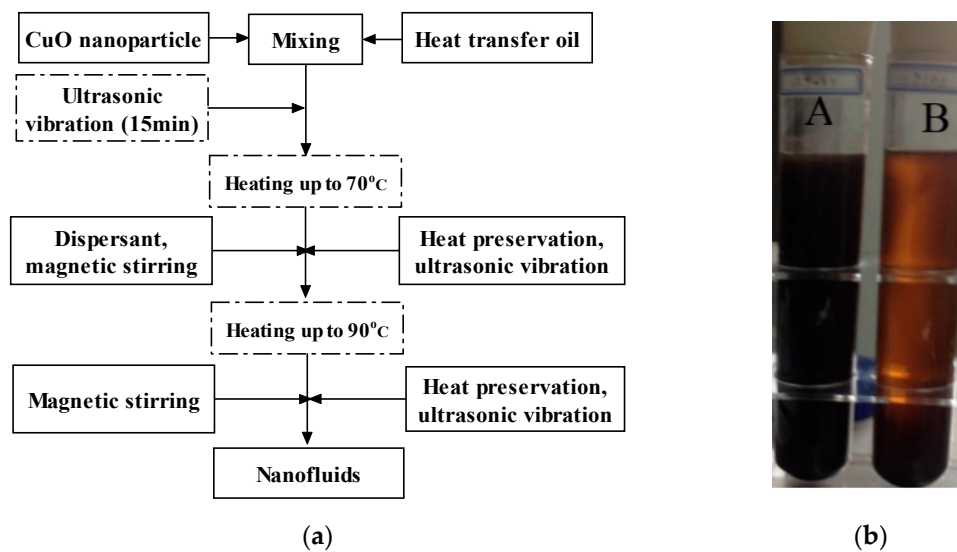


**Figure 3.** Nanofluids-preparing process. (a) The “two-step” method (additional steps are shown by dotted boxes). (b) Prepared nanofluids after a 3-day settling test at room temperature. A in (b) represents the modified two-step method, and (B) in (b) represents a conventional two-step method discussed in the literature [36].

## 2.2. Thermal Impulse Testing

In a medium-temperature solar thermal collector, the average operation temperature is typically greater than 80 °C, but at night and on cloudy days, the collector (and the working fluid, if not drained) cools to the ambient temperature. To simulate this heating/cooling cycle, the prepared nanofluids samples were heated while stirring with a magnetic heating/stirring sleeve. After the desired temperature was held for a desired time frame, the samples were cooled to room temperature with a water bath. This heating and cooling process was repeated for numerous cycles to simulate the expected operational temperature range of the working fluid. Upon the completion of thermal cycle tests, the treated nanofluids were allowed to settle for three days at ambient conditions, before their stability was assessed. Observation, sedimentation time, and optical transmittance were used as measures of nanofluids stability. Among these measurements, the transmittance measurement was most sensitive and most quantifiable, wherein the increased transmittance indicated a loss of stability (i.e., agglomeration and settling of particles). The transmittance was measured with a UV-IR spectrometer, a Lambda 950.

The experiment was repeated with different heating cycles to explore the effects of thermal impulse cycles on the stability of CuO/oil nanofluids. Here, the numbers of heating cycles were set to 5, 10, 25, and 45, with a working temperature of 100 °C. The results of these tests are shown in Figure 4, illustrating that the agglomeration of nanofluids was obviously accelerated by multiple heating cycles. At the same time, it was found that the agglomerations of samples 1 and 2 were similar. Samples 3 and 4 also yielded similar (nearly complete loss of the particle suspension) results.

In addition to normal operational thermal cycles, other aspects of the system can also affect stability. Exposure to light and temporary high temperatures can also be detrimental to direct-absorption working fluids. Therefore, the effects of the maximum working temperatures on stability were also investigated by heating these CuO/oil nanofluids up to 80, 100, 120, and 150 °C. In this case, 10 heating cycles were used, with the maximum temperature of each cycle maintained for 10 min. The transmittances of four samples for this test are shown in Figure 5, indicating that all heated samples aggregated significantly (e.g., much higher transmittance across the whole spectrum) relative to the unheated nanofluids sample 5, which was kept at room temperature. It is obvious that heating can deteriorate nanofluids optical properties, and the higher the heating temperature, the more obvious the agglomeration of nanofluids.

For sample 4, the settling time test revealed that almost all of the particles settled within five hours after heating to 150 °C.

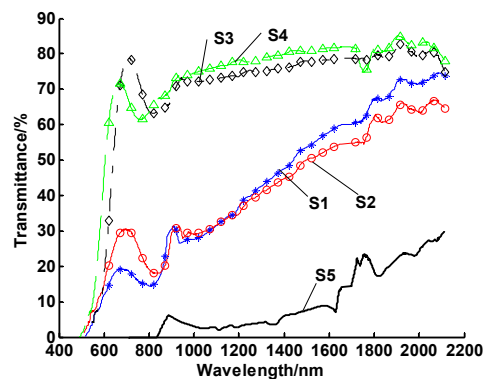


**Figure 4.** Spectral transmittances of CuO/oil nanofluids for a number of thermal cycles. Note: samples 1–4 experienced 5, 10, 25, and 45 thermal cycles, respectively, while sample 5 underwent no thermal cycle.

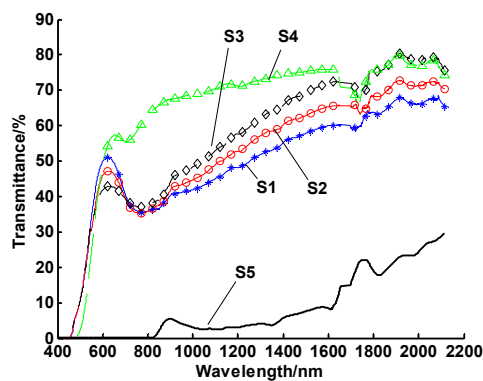


**Figure 5.** Spectral transmittances of CuO/oil nanofluids at different maximum temperatures. Note: samples 1–4 were tested at the maximum test temperatures of 80, 100, 120, and 150 °C, respectively, while sample 5 was kept at room temperature.

To explore the effect of heating time, nanofluids was heated to 100 °C and held at this temperature for variable time frames (5, 10, 30, and 60 min). The number of heating cycles was still set to 10. The results are shown in Figure 6. It can be seen that, as heating time increased, agglomeration also increased.

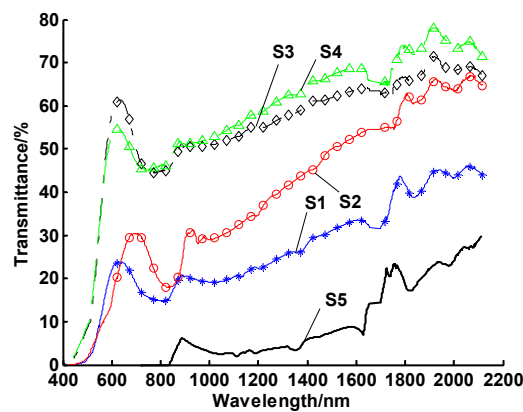


**Figure 6.** Spectral transmittances of nanofluids with different heating times. Note: samples 1–4 were tested for heating times of 5, 10, 30, and 60 min, respectively, while sample 5 experienced no heating.

Overall, the dispersion stabilities of these nanofluids were poor. This can be explained by the fact that at higher temperatures, nanoparticles have more probability of colliding (i.e., due to increased Brownian motion) and, upon collision, the ratio between attraction force and repulsion force increases (i.e., a function of  $k_B T$  [37]). In addition, the higher the temperature, the lower the viscosity of the base fluid (e.g.,  $v = CT + B$ , where  $v$  is the viscosity of the nanofluids,  $T$  is the temperature of nanofluids, and  $C$  and  $B$  are constants) [38], which enables a faster settling rate for agglomerated particles. Lastly, heating also accelerates the decomposition of oleic acid and the oxidation of the heat transfer oil, both of which are dependent on temperature.

### 3. Optimization of Preparation Processes

According to the DLVO theory, the dispersion of nanoparticles in a base fluid is mainly based on the steric stability mechanism. In general, steric stability can be controlled by the particle type, the base fluid type, and the dispersant type, and the relative concentrations of these particles as well as the pH value of the base liquid. For oil-based nanofluids, changing pH value is not suitable, because strong acids and bases can break the organic bonds of base fluids. Therefore, for a given fluid/particle combination, the main degree of freedom is in the addition of a dispersant, making sure the initial physical dispersion (including magnetic stirring and ultrasonic vibration) is effective.

#### 3.1. Experimental Study on the Optimal Dispersant

Due to the fact that a base fluid is a nonpolar substance and a dispersant should have thermal chemical stability, four kinds of dispersants were selected: oleic acid, glycerol monostearate, Span 80, and Tween 40. The properties of each dispersant are shown in Table 2. In Table 2, the hydrophile lipophile balance (HLB) is provided, which represents the hydrophilic and oil hydrophilic equilibrium value. The abbreviations “AR” and “CP” were used to indicate analytical purity and chemical purity, respectively. The result of using each dispersant, after 30 days of settling, is shown in Figure 7.



**Figure 7.** Photo of nanofluids with different dispersants after 30 days of settling time: (a) oleic acid; (b) glyceryl monostearate; (c) Span 80; (d) Tween 40.

**Table 2.** Properties of dispersants.

Dispersants	Oleic Acid	Glyceryl Monostearate	Span 80	Tween 40
Chemical formula	$C_{18}H_{34}O_2$	$C_{21}H_{42}O_4$	$C_{24}H_{44}O_6$	$C_{22}H_{42}O_6$
Density (20 °C)	0.891 g/mL	0.985 g/cm <sup>3</sup>	0.994 g/mL	1.10 g/mL
Boiling point	350–360 °C	476.9 °C	579.3 °C	—
Melting point	13.4 °C	80 °C	11 °C	0.1 °C
Hydrophile lipophile balance (HLB)	1.0	3.8	4.3	5.6
Purity	AR	CP	CP	CP

It should be noted that if the HLB value is higher, as indicated by the name, there are less hydrophilic groups. Figure 7 shows that oleic acid, which had the highest hydrophilicity, resulted in the best dispersion and that Tween 40 had the worst dispersion effect. Thus, the results roughly aligned with the respective HLB values of the dispersants. Since glycerol monostearate is solid at room temperature, some large particles condensed upon cooling, as shown in Figure 7b, which resulted in particle agglomeration. Therefore, oleic acid was selected as a dispersant of nanofluids in subsequent experiments.

### 3.2. Experimental Study on the Optimal Concentration of the Dispersant

Six groups of 100 mL CuO/oil ( $v_{CuO}: v_{oil} = 1:99$ ) nanofluids were prepared with different amounts of the dispersant oleic acid (from 0 mL to 1.5 mL with a 0.25 mL interval), each of which underwent a one hour ultrasonic vibration time and a settling time of 30 days. Because the stratification of some samples was not obvious, the transmittance, shown in Figure 8, was used to evaluate stability.

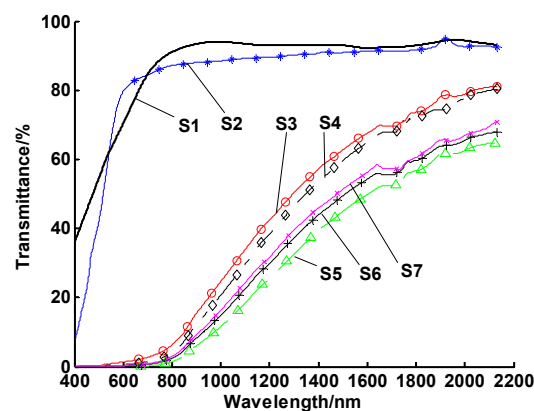


**Figure 8.** Spectral transmittances of CuO/oil nanofluids with different oleic acid volumes. Note: samples 1–7 had different oleic acid volumes from 0 mL to 1.5 mL with a 0.25 mL interval, respectively.

Figure 8 shows that the optimum oleic acid content was 1 mL. The reason is that when the amount of oleic acid was low (i.e., S1 = 0 or S2 = 0.25 mL in Figure 8, the CuO particles were not fully coated so they agglomerated and fell out of suspension, resulting in high UV-Vis transmittance. On the other hand, when superfluous unabsorbed oleic acid was present, the molecular chain could reunite through a bridging action, which led to flocculation and deterioration of stability.

### 3.3. Experimental Study on the Optimal Ultrasonic Time

Six groups of 100 mL CuO/oil ( $v_{CuO}: v_{oil} = 1:99$ ) nanofluids (using 1 mL of oleic acid) were prepared with different ultrasonic times (from 0.5 to 3 h with a 0.5 h intervals) and left to settle for 30 days. The measurement results are shown in Figure 9.

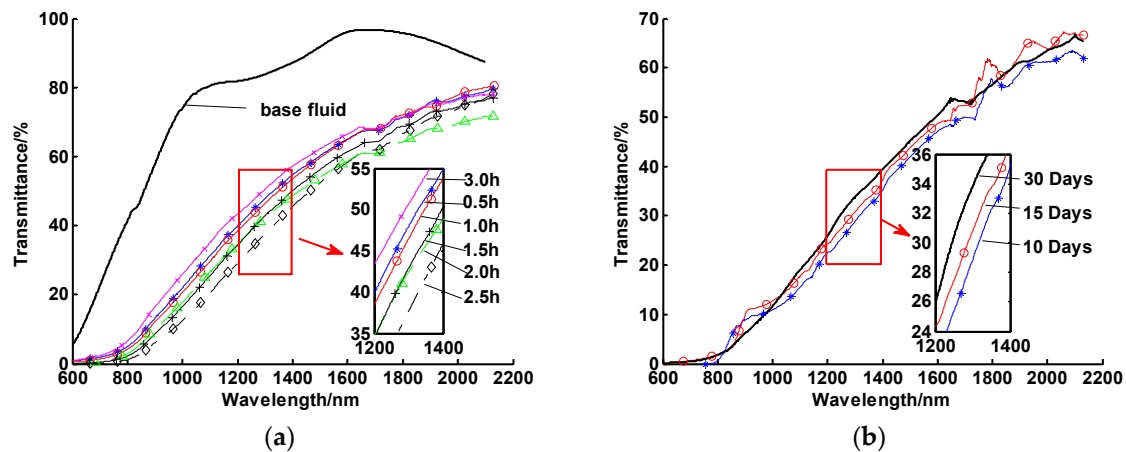


**Figure 9.** Spectral transmittances of CuO/oil nanofluids for (a) different periodic resonication times and (b) different settling times (10, 15, and 30 days).

Figure 9a shows that the best ultrasonic vibration time was 1.5 h. Ultrasonic vibration produces high-frequency mechanical waves, which can effectively restrain the agglomeration of particles. If the ultrasonic time is too short, the initial soft particle agglomerations stored in a powder form will not be completely broken, which leads to fast sedimentation. On the other hand, if the ultrasonic time is too long, the internal energy and temperature of the sample increase, increasing the risk of particle–particle collisions and agglomeration. According to the single-factor analysis above, CuO/oil nanofluids were prepared with an optimal concentration of the dispersant for different ultrasonic times and left to settle for 10, 15, and 30 days. The transmittances at room temperature with different settling times are displayed in Figure 9b. It can be seen that there is no obvious difference among these three transmittance curves, which indicated that the stability at room temperature was quite good and could be extended to more than 30 days.

### 3.4. Orthogonal Tests

An orthogonal test provides a systematic experimental method to study many factors and levels to find the optimum combination of several factors. The design of an orthogonal experiment was based on an orthogonal table. Based on the tests and analysis, the factors in the orthogonal test are as follows: (A) nanoparticle diameter, (B) nanoparticle concentration, (C) type of dispersant, and (D) periodic resonication time. In order to improve the thermal stability of nanofluids, each sample was treated with ultrasonic vibration after heating cycles. The corresponding ultrasonic vibration time was called “periodic resonication time” here. The levels of the factors and the orthogonal experimental design are shown in Tables 3 and 4. The precipitation time was defined by the time that nanofluids were delaminated to a specified height. According to the orthogonal experimental table, nanofluids were prepared, and the precipitation time of the nanofluids was recorded with a heating temperature of 150 °C, a heating time of five minutes, and 10 heating cycles.

**Table 3.** Factor levels.

Level	Diameter (A)	Concentration (B)	Dispersant (C)	Periodic Resonication Time (D)
1	100 nm	3 vol%	Oleic acid	2 h
2	60 nm	2 vol%	Oleic acid + Span 80	0.5 h
3	30 nm	1 vol%	Span 80	0 h

**Table 4.** Orthogonal experimental design and range analysis.

Items	A	B	C	D	Results
1	1	1	1	1	19
2	1	2	2	2	16
3	1	3	3	3	12
4	2	1	2	3	16
5	2	2	3	1	32
6	2	3	1	2	24
7	3	1	3	2	15
8	3	2	1	3	24
9	3	3	2	1	50
$k_1$	47	50	67	101	
$k_2$	72	72	82	55	
$k_3$	89	86	59	52	
$\bar{k}_1$	15.7	16.7	22.3	33.7	
$\bar{k}_2$	24	24	27.3	18.3	
$\bar{k}_3$	29.7	28.7	19.7	17.3	
Range	14	12	7.6	16.4	

Note:  $k_i$  ( $i = 1, 2, 3$ ) and  $\bar{k}_i$  ( $i = 1, 2, 3$ ) represent ranges and average ranges at different levels.

In order to study the results from orthogonal tests, range analysis was utilized in this study. Range analysis is a statistical method to determine the factor sensitivity to experimental results according to orthogonal experiments. The range is defined as a distance between the extreme values of data. The greater the range is, the more sensitive the factor is. The mean principal effects of each factor were obtained by Minitab analysis, as shown in Figure 10.

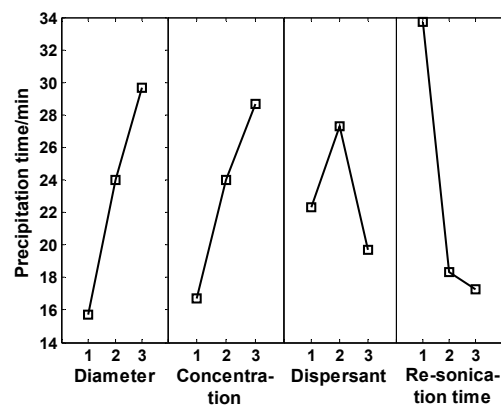
**Figure 10.** Effects of four key factors.

Figure 10 shows that the four factors above had obvious effects on the degradation rate of nanofluids under the condition of heating impulse. The reasons are as follows: (1) the larger the particle size, the greater the attractive potential energy and gravity between particles, and the easier the settlement; (2) with the increase of the concentration of nanoparticles, the distance between particles decreased, the interactions between particles were strengthened, and the agglomeration occurred more easily; (3) the structure of oleic acid molecule was serrated, while normal CuO nanoparticles were spherical and therefore the coating was not dense enough. Span 80 is a good oil-in-water dispersant with more stable properties. Oleic acid and Span 80 were used together, and the coating effect was better; (4) periodic ultrasonic vibration can break agglomeration caused by heating. By analyzing the range analysis of orthogonal tests in Table 3, we can get the main order of each influencing factor as follows: periodic re-sonication time > particle size > concentration > dispersant. In addition, the orthogonal experiment results showed that the nanofluids tended to agglomerate very quickly under

conditions of medium temperatures or thermal cycles, in spite of the fact that the nanofluids had more than 30-day stability at room temperature, which indicated that stability under medium or high temperatures was quite difficult to maintain and different from that under room temperature.

#### 4. Experiment on Thermal Properties of CuO/Oil Nanofluids

##### 4.1. Experiment on the Thermal Conductivity of CuO/Oil Nanofluids

The thermal conductivity of oil-based CuO nanofluids can be used as a heat transfer medium to measure its heat-collecting effect. Moreover, the agglomeration and precipitation of nanoparticles make the thermal conductivity worse, as the stability becomes worse. Therefore, the thermal conductivity and stability of the fluids were investigated by measuring and comparing the thermal conductivities with an outdoor absorption heat collection experiment.

The thermal conductivity coefficient of nanofluids is a key parameter in the studies of the thermal properties of nanofluids. The main methods to measure the thermal conductivities of liquids include the heat probe method, steady-state plate method, and transient hot wire method. The third is the best method. In this paper, a TC3000E thermal conductivity meter, which used the transient hot wire method, was adopted to measure CuO/oil nanofluids.

CuO/oil nanofluids with volume fractions (0.05%, 0.1%, and 0.2%) were prepared, and their thermal conductivities were measured as shown in Figure 11a. Yamada and Ota put forward a model equation based on an effective medium theory in 1980, which was written as Equation (2):

$$\frac{k_{nf}}{k_{bf}} = \frac{k_p + Kk_{bf} + K(k_p - k_{bf})\varphi}{k_p + Kk_{bf} - (k_p - k_{bf})\varphi}, \quad (2)$$

where  $k_p$  and  $k_{bf}$  represent the coefficient of thermal conductivity of CuO particles and the coefficient of thermal conductivity of a base fluid,  $k_{nf}$  is the coefficient of thermal conductivity of the mixture. The parameter  $K$  is related to the volume fraction and the shape of particles. When the particle is spherical, the parameter  $K$  can be written as [39]:

$$K = 2\varphi^{-0.2}. \quad (3)$$

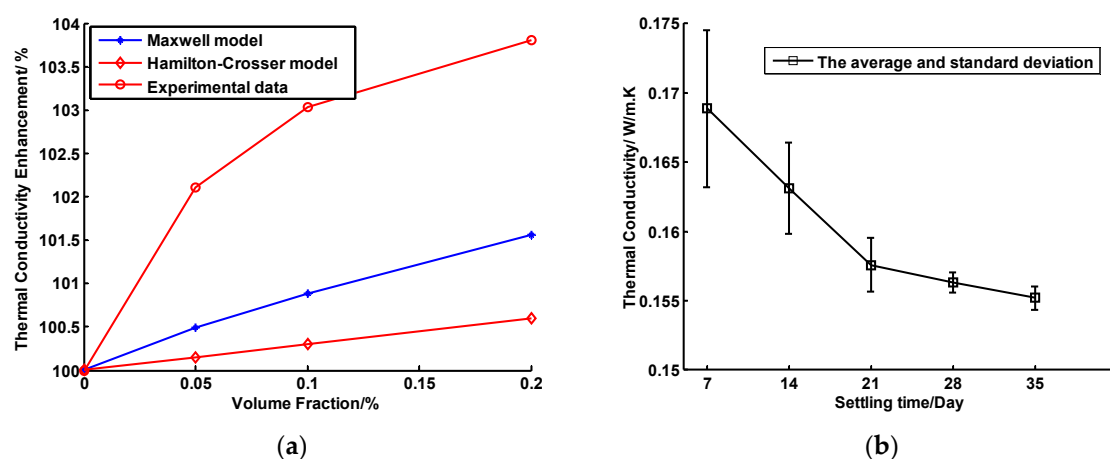


**Figure 11.** (a) Theoretical and tested values of thermal conductivities of nanofluids as a function of volume fraction. (b) Thermal conductivity of nanofluids as a function of settling time.

The thermal conductivities of CuO nanofluids stored in different days are shown in Figure 11b. It can be seen from Figure 11b that the thermal conductivity of fluids decreased rapidly in the first three weeks and decreased slowly in the fourth and fifth weeks.

The experimental results showed that the thermal conductivity of CuO/oil nanofluids slowly increased with the increase of volume fraction. For example, the thermal conductivity of CuO/oil nanofluids with a 0.2% volume fraction was 3.8% higher than that of the base fluid. In addition, the thermal conductivity of nanofluids decreased by about 8.1% with the settling time increased from 7 to 35 days.

#### 4.2. Photothermal Conversion of CuO/oil Nanofluids

There have been many studies on the enhancement of heat transfer performance of nanofluids, but few studies focused on the absorption performance of solar energy. In the paper, CuO/oil nanofluids were applied to a solar energy collector to conduct a direct absorption heat collection experiment, investigate its photothermal conversion efficiency and temperature rise speed and verify its enhancement effects on solar radiation absorption and photothermal conversion performance.

In the experiment, a Fresnel solar concentrator, shown in Figure 12, was used to conduct concentrated heat. Its main parameters are shown in Table 5. The concentrator was composed of microarc mirrors, a tracking device, and a support structure. The microarc mirrors were placed in the north–south direction, and the sunlight was concentrated on the heat collector plate at the focal line position. The parallelogram mechanism was used to control the mirrors to track the sun and improve the heat collection efficiency of the system.

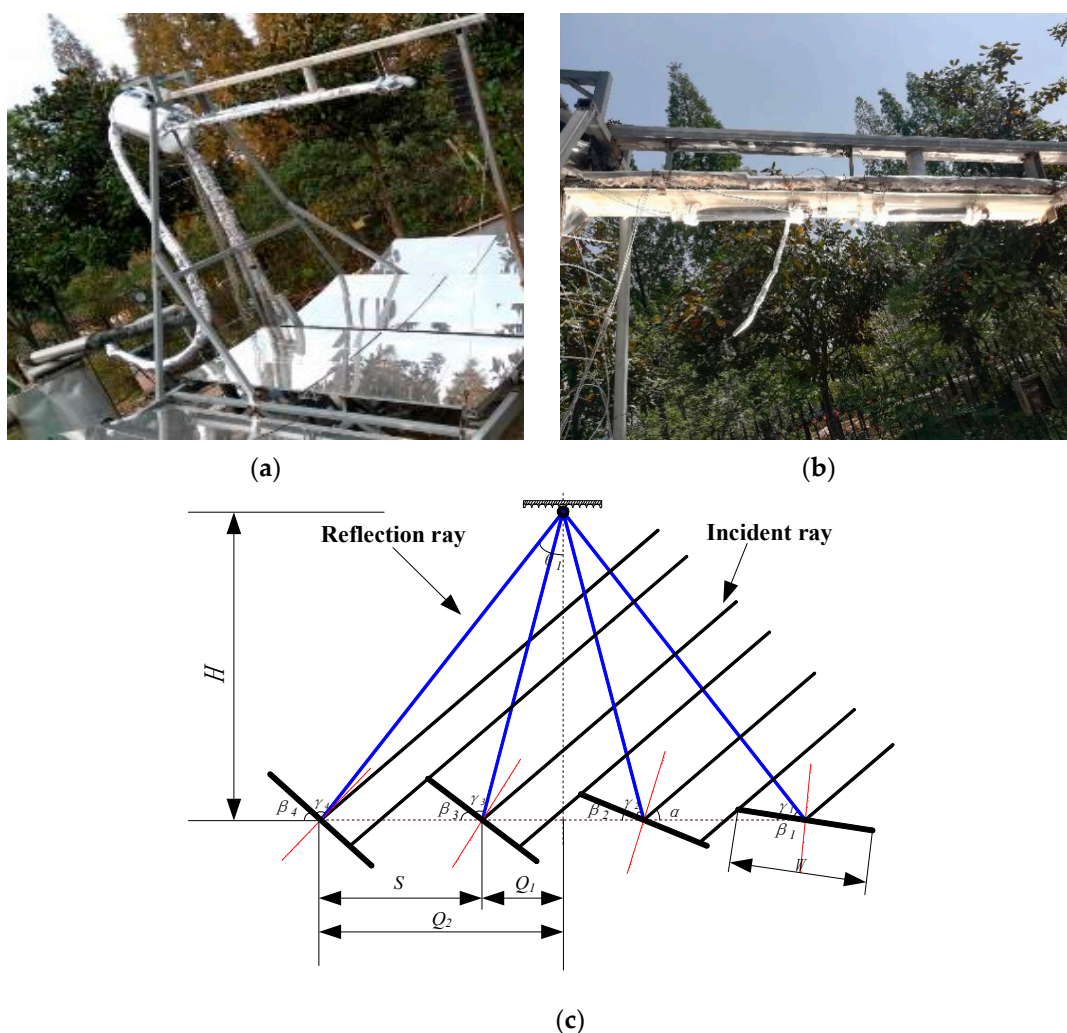


**Figure 12.** Linear Fresnel solar collector: (a) overview image; (b) solar evacuated tube with nanofluids; (c) schematic diagram.

**Table 5.** Parameters of the Fresnel solar collector.

Parameter	Value
Mirror width $W$ (mm)	800
Mirror length $L$ (mm)	2200
$Q_1$ (mm)	475
Center distance $S$ (mm)	950
Collector height $H$ (mm)	1800
Tilt angle ( $^\circ$ )	32

Solar evacuated tubes with a length of 50 cm and a diameter of 4.7 mm, made by high-boron glass, were used to collect solar heat. CuO/oil nanofluids worked as working fluids with an uncoated solar evacuated tube, while heat transfer oil worked as a working fluid with a coated solar evacuated tube for comparison. The direct solar radiation intensity was measured by a Newport 1918-R optical power meter. The temperatures of stagnant working fluids and tube walls were measured by thermocouples, and the temperature rise rates of different working fluids, the temperature changes of the outer walls of the tubes, and the instantaneous heat collection efficiencies were compared. The instantaneous photothermal conversion efficiency was calculated by Equation (4):

$$\eta = \frac{mC_p(T_{i+1} - T_i)}{GA\Delta t}, \quad (4)$$

where  $\eta$  is the instantaneous heat collection efficiency,  $m$  and  $C_p$  represent the quality of nanofluids (kg) and specific heat (J/(kg·°C)), respectively,  $T_{i+1}-T_i$  represents the temperature difference,  $A$  is the lighting area of a collector tube,  $G$  is the average irradiance of concentrated incident rays, and  $\Delta t$  is the time interval. The mass and specific heat capacity of the prepared nanofluids were similar to those of the thermal conductive oil due to their low concentrations.

The experiment was conducted in Nanjing (119 °E, 32 °N), and the test time was April 8 2018. The test period was from 11:00 a.m. to 11:30 a.m. Due to uncontrollable weather conditions, the irradiance of the sun after concentrating light fluctuated within a certain range (2000–5000 W/m<sup>2</sup>).

CuO/oil nanofluids with a 0.2% volume fraction were prepared and filled in a solar evacuated tube. The temperature rise of CuO/oil nanofluids and the outer tube wall are shown in Figure 13. The temperature of CuO/oil nanofluids was increased from 20.8 to 129.0 °C, and the temperature of the outer tube wall was increased from 21.8 to 62.2 °C within 30 min. It was found that the temperature rate in the beginning was quite large due to good thermal conductivity of CuO/oil nanofluids. The instantaneous thermal efficiencies of CuO/oil nanofluids at different times were calculated. The result showed that the efficiency of CuO/oil nanofluids was 67.6% at 11:05 a.m. and decreased to 36.3% at 11:30 a.m., while the thermal efficiencies with the working fluid of heat transfer oil was 51.3% in the beginning and 42.9% at 11:30 a.m. It was found that nanofluids had good optical properties when the working temperature was lower than 110 °C. The reason is that heat radiation loss of nanofluids became the main source with increase of working temperature.

Therefore, due to high thermal conductivity of nanofluids, nanofluids could be good working fluids for solar systems. However, in spite of the fact that a fluid is stable at room temperature, which is often done in the literatures, it does not mean that it will actually work in real applications. Periodic resonication can help, but it is not enough to achieve a useful service life. In addition, heat radiation loss also should be decreased.

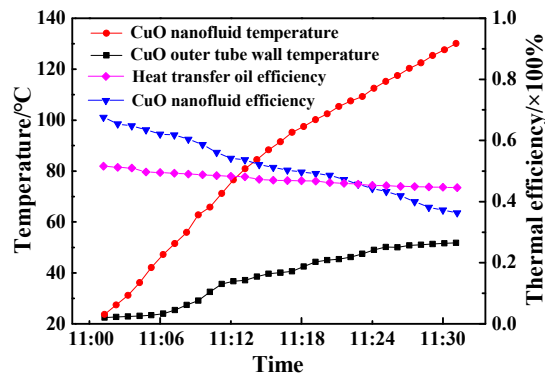


**Figure 13.** Temperature and instantaneous thermal efficiency curves of CuO/oil nanofluids and the outer tube wall as a function of time.

## 5. Conclusions

This study experimentally showed the effects of working conditions on the stability of CuO/oil nanofluids. To improve the stability, the effects of preparation processes were investigated and optimized with an orthogonal test. The coefficient of thermal conductivity of nanofluids and the thermal performance working as working fluids in a solar collector were also presented. The following points have been discovered:

1. Heating temperature, heating cycles, and heating time were all found to significantly influence the stability of nanofluids;
2. Nanofluids tended to aggregate quickly at medium temperatures or after several thermal cycles, even if they had high stability at room temperature (e.g., more than 30 days without settling).
3. According to our orthogonal test, the main factors affecting thermal impulse stability were the periodic resonication time, particle size, particle concentration, and the type of dispersant;
4. The thermal conductivity of CuO/oil nanofluids with a 0.2% volum fraction was 3.8% higher than that of the pure oil base fluid, enabling its thermal efficiency in the solar collector to achieve 67.6%.

Overall, physical treatment on nanoparticles can realize long-term stability of nanofluids at room temperature but can only marginally improve the thermal impulse stability. Chemical treatment methods (e.g., attaching functional groups with high bond energy [21]) are needed to maintain high-temperature stability of nanofluids, and long-term thermal stability of nanofluids for practical applications is still a big challenge.

**Author Contributions:** Conceptualization, M.Y. and S.W.; methodology, M.Y. and R.A.T.; software, S.W. and Y.W.; validation, M.Y. and S.W.; formal analysis, M.Y. and R.A.T.; investigation, M.Y. and R.A.T.; resources, Y.Z.; data curation, S.W. and M.Y.; writing of the original draft preparation, M.Y., S.W., and R.A.T.; writing of review and editing, R.A.T. and M.A.M. All authors have read and agreed to the published version of the manuscript.

**Funding:** This research was funded by six talent peaks projects in Jiangsu, China (grant number: XNY-028), the National Key Research and Development Program of China (grant number: 2018YFB1502900), the National Natural Science Foundation of China (grant number: 51105192), the China Postdoctoral Science Foundation (grant number: 2018M632294), and major projects of natural science research in Jiangsu higher education institutions (grant number: 17KJA470004).

**Conflicts of Interest:** The authors declare no conflicts of interest.

## References

1. Tehrani, S.S.M.; Taylor, R.A. Off-Design Simulation and Performance of Molten Salt Cavity Receivers in Solar Tower Plants under Realistic Operational Modes and Control Strategies. *Appl. Energy* **2016**, *179*, 698–715. [[CrossRef](#)]

2. Otanicar, T.P.; Theisen, S.; Norman, T.; Tyagi, H.; Taylor, R.A. Envisioning Advanced Solar Electricity Generation: Parametric Studies of CPV/T Systems with Spectral Filtering and High Temperature PV. *Appl. Energy* **2015**, *140*, 224–233. [[CrossRef](#)]
3. Menbari, A.; Alemrajabi, A.A.; Ghayeb, Y. Investigation on the Stability, Viscosity and Extinction Coefficient of CuO–Al<sub>2</sub>O<sub>3</sub>/Water Binary Mixture Nanofluid. *Exp. Therm. Fluid Sci.* **2016**, *74*, 122–129. [[CrossRef](#)]
4. Aguilar, T.; Navas, J.; Sánchez-Coronilla, A.; Martín, E.I.; Gallardo, J.J.; Martínez-Merino, P.; Gómez-Villarejo, R.; Piñero, J.C.; Alcántara, R.; Fernández-Lorenzo, C. Investigation of Enhanced Thermal Properties in NiO-Based Nanofluids for Concentrating Solar Power Applications: A Molecular Dynamics and Experimental Analysis. *Appl. Energy* **2018**, *211*, 677–688. [[CrossRef](#)]
5. Sharafeldin, M.A.; Gróf, G. Efficiency of Evacuated Tube Solar Collector Using WO<sub>3</sub>/water Nanofluid. *Renew. Energy* **2019**, *134*, 453–460. [[CrossRef](#)]
6. Du, M.; Tang, G.H. Optical Property of Nanofluids with Particle Agglomeration. *Sol. Energy* **2015**, *122*, 864–872. [[CrossRef](#)]
7. Yousefi, T.; Veysi, F.; Shojaeizadeh, E.; Zinadini, S. An Experimental Investigation on the Effect of Al<sub>2</sub>O<sub>3</sub>–H<sub>2</sub>O Nanofluid on the Efficiency of Flat-Plate Solar Collectors. *Renew. Energy* **2012**, *39*, 293–298. [[CrossRef](#)]
8. Mohammad, S.; Mohammad, P.F.; Saeed, Z.H. Experimental Investigation of the Effects of Silica/water Nanofluid on PV/T (photovoltaic thermal units). *Energy* **2014**, *66*, 264–272. [[CrossRef](#)]
9. Taylor, R.A.; Phelan, P.E.; Otanicar, T.P.; Walker, C.A.; Nguyen, M.; Trimble, S.; Prasher, R. Applicability of Nanofluids in High Flux Solar Collectors. *J. Renew. Sustain. Energy* **2011**, *3*. [[CrossRef](#)]
10. Amiri, A.; Øye, G.; Sjöblom, J. Temperature and Pressure Effects on Stability and Gelation Properties of Silica Suspensions. *Colloid Surf. A-Physicochem. Eng. Asp.* **2011**, *378*, 14–21. [[CrossRef](#)]
11. Mahbulbul, I.M.; Saidur, R.; Amalina, M.A.; Niza, M.E. Influence of Ultrasonication Duration on Rheological Properties of Nanofluid: An Experimental Study with Alumina–water Nanofluid. *Int. Commun. Heat Mass Transf.* **2016**, *76*, 33–40. [[CrossRef](#)]
12. Li, F.S.; Li, L.; Zhong, G.J.; Zhai, Y.L.; Li, Z.H. Effects of Ultrasonic Time, Size of Aggregates and Temperature on the Stability and Viscosity of Cu-Ethylene Glycol (EG) Nanofluids. *Int. J. Heat Mass Transf.* **2019**, *129*, 278–286. [[CrossRef](#)]
13. Khairul, M.A.; Shah, K.; Doroodchi, E.; Azizian, R.; Moghtaderi, B. Effects of Surfactant on Stability and Thermo-Physical Properties of Metal Oxide Nanofluids. *Int. J. Heat Mass Transf.* **2016**, *98*, 778–787. [[CrossRef](#)]
14. Sezer, N.; Koç, M. Stabilization of the Aqueous Dispersion of Carbon Nanotubes Using Different Approaches. *Therm. Sci. Eng. Prog.* **2018**, *8*, 411–417. [[CrossRef](#)]
15. Nagarajan, P.K. Influence of Stability and Particle Shape Effects for an Entropy Generation Based Optimized Selection of Magnesia Nanofluid for Convective Heat Flow Applications. *Appl. Surf. Sci.* **2019**, *489*, 560–575. [[CrossRef](#)]
16. Arulprakasajothi, M.; Elangovan, K.; HemaChandraReddy, K.; Suresh, S. Heat Transfer Study of Water-based Nanofluids Containing Titanium Oxide Nanoparticles. *Mater. Today: Proc.* **2015**, *2*, 3648–3655. [[CrossRef](#)]
17. Bashirnezhad, K.; Bazri, S.; Safaei, M.R.; Goodarzi, M.; Dahari, M.; Mahian, O.; Dalkılıç, A.S.; Wongwisese, S. Viscosity of Nanofluids: A Review of Recent Experimental Studies. *Int. Commun. Heat Mass Transf.* **2016**, *73*, 114–123. [[CrossRef](#)]
18. Li, Y.J.; Eric, S.; Simon, T.; Xi, S.Q.; Zhou, J.E. A Review on Development of Nanofluid Preparation and Characterization. *Powder Technol.* **2009**, *196*, 89–101. [[CrossRef](#)]
19. Al-Gebory, L.; Mengüç, M.P. The Effect of PH on Particle Agglomeration and Optical Properties of Nanoparticle Suspensions. *J. Quant. Spectrosc. Radiat. Transf.* **2018**, *219*, 46–60. [[CrossRef](#)]
20. Sharma, S.K.; Gupta, S.M. Preparation and Evaluation of Stable Nanofluids for Heat Transfer Application: A Review. *Exp. Therm. Fluid Sci.* **2016**, *79*, 202–212. [[CrossRef](#)]
21. Taylor, R.A.; Hjerrild, N.; Duhaini, N.; Pickford, M.; Mesgari, S. Stability Testing of Silver Nanodisc Suspensions for Solar Applications. *Appl. Surf. Sci.* **2018**, *455*, 465–475. [[CrossRef](#)]
22. Hordy, N.; Rabilloud, D.; Meunier, J.L.; Coulombe, S. High Temperature and Long-Term Stability of Carbon Nanotube Nanofluids for Direct Absorption Solar Thermal Collectors. *Sol. Energy* **2014**, *105*, 82–90. [[CrossRef](#)]
23. Bellos, E.; Tzivanidis, C. A Review of Concentrating Solar Thermal Collectors with and without Nanofluids. *J. Therm. Anal. Calorim.* **2019**, *135*, 763–786. [[CrossRef](#)]
24. Bellos, E.; Tzivanidis, C. Multi-Criteria Evaluation of a Nanofluid-Based Linear Fresnel Solar Collector. *Sol. Energy* **2018**, *163*, 200–214. [[CrossRef](#)]

25. Sani, E.; Barison, S.; Pagura, C.; Mercatelli, L.; Sansoni, P.; Fontani, D.; Jafrancesco, D.; Francini, F. Carbon Nanohorns-Based Nanofluids as Direct Sunlight Absorbers. *Opt. Express* **2010**, *18*, 5179–5187. [[CrossRef](#)]
26. Mesgari, S.; Coulombe, S.; Hordy, N.; Taylor, R.A. Thermal Stability of Carbon Nanotube-Based Nanofluids for Solar Thermal Collectors. *Mater. Res. Innov.* **2015**, *19*. [[CrossRef](#)]
27. Jiang, H.F.; Li, H.; Zan, C.; Wang, F.Q.; Yang, Q.P.; Shi, L. Temperature Dependence of the Stability and Thermal Conductivity of an Oil-Based Nanofluid. *Thermochim. Acta* **2014**, *579*, 27–30. [[CrossRef](#)]
28. Otanicar, T.; Hoyt, J.; Fahar, M.; Jiang, X.; Taylor, R.A. Experimental and Numerical Study on the Optical Properties and Agglomeration of Nanoparticle Suspensions. *J. Nanopart. Res.* **2013**, *15*, 2039. [[CrossRef](#)]
29. Mesgari, S.; Taylor, R.A.; Crisostomo, F.; Li, Q.; Hjerrild, N.E.; Scott, J. An Investigation of Thermal Stability of Carbon Nanofluids for Solar Thermal Applications. *Sol. Energy Mater. Sol. Cells* **2016**, *157*, 652–659. [[CrossRef](#)]
30. Khanafer, K.; Vafai, K. A Review on the Applications of Nanofluids in Solar Energy Field. *Renew. Energy* **2018**, *123*, 398–406. [[CrossRef](#)]
31. Sezer, N.; Atieh, M.A.; Koç, M. A Comprehensive Review on Synthesis, Stability, Thermophysical Properties, and Characterization of Nanofluids. *Powder Technol.* **2019**, *344*, 404–431. [[CrossRef](#)]
32. Xu, G.Y.; Chen, W.; Deng, S.M.; Zhang, X.S.; Zhao, S.N. Performance Evaluation of a Nanofluid-Based Direct Absorption Solar Collector with Parabolic Trough Concentrator. *Nanomaterials* **2015**, *5*, 2131–2147. [[CrossRef](#)]
33. Mwesigye, A.; Huan, Z.J.; Meyer, J.P. Thermodynamic Optimisation of the Performance of a Parabolic Trough Receiver Using Synthetic Oil-Al<sub>2</sub>O<sub>3</sub> Nanofluid. *Appl. Energy* **2015**, *156*, 398–412. [[CrossRef](#)]
34. Okonkwo, E.C.; Essien, E.A.; Akhayere, E.; Abid, M.; Kavaz, D.; Ratlamwala, T.A.H. Thermal Performance Analysis of a Parabolic Trough Collector Using Water-Based Green-Synthesized Nanofluids. *Sol. Energy* **2019**, *170*, 658–670. [[CrossRef](#)]
35. Dardan, E.; Afrand, M.; Isfahani, A.H.M. Effect of Suspending Hybrid Nano-Additives on Rheological Behavior of Engine Oil and Pumping Power. *Appl. Therm. Eng.* **2016**, *109*, 524–534. [[CrossRef](#)]
36. Yang, L.; Hu, Y. Toward TiO<sub>2</sub> Nanofluids-Part 1: Preparation and Properties. *Nanoscale Res. Lett.* **2017**, *12*, 417. [[CrossRef](#)]
37. Priya, K.R.; Suganthi, K.S.; Rajan, K.S. Transport Properties of Ultra-Low Concentration CuO-Water Nanofluids Containing Non-Spherical Nanoparticles. *Int. J. Heat Mass Transf.* **2012**, *55*, 4734–4743. [[CrossRef](#)]
38. Kim, H.J.; Lee, S.H.; Lee, J.H.; Jang, S.P. Effect of Particle Shape on Suspension Stability and Thermal Conductivities of Water-Based Bohemite Alumina Nanofluids. *Energy* **2015**, *90*, 1290–1297. [[CrossRef](#)]
39. Yang, L.; Xu, J.; Zhang, X. Recent Developments on Viscosity and Thermal Conductivity of Nanofluids. *Powder Technol.* **2017**, *317*, 348–369. [[CrossRef](#)]



© 2020 by the authors. Licensee MDPI, Basel, Switzerland. This article is an open access article distributed under the terms and conditions of the Creative Commons Attribution (CC BY) license (<http://creativecommons.org/licenses/by/4.0/>).